ChemPubSoc Europe

DOI: 10.1002/cctc.201501069

CHEMCATCHEM
Full Papers

Ruthenium Nanoparticles in High-Throughput Studies of Chemoselective Carbonyl Hydrogenation Reactions

Julia Gmeiner,[a] Silke Behrens,[b] Bernd Spliethoff,[c] and Oliver Trapp*[a]

Small (≤1.4 nm) and very active Ru nanoparticles, stabilized in a polysiloxane matrix, were prepared and studied in hydrogenation reactions by the integration of catalysis and analysis. We used our strategy to combine catalytic activity and separation selectivity in a capillary microreactor, installed in a GC–MS instrument, to develop a fast and reliable screening tool for catalysis over Ru nanoparticles. A high conversion using a low catalyst loading of 0.3 mol% and temperature and long-term stability of the catalytically active column were observed for the hydrogenation of various carbonyl compounds, which included aldehydes, ketones, and pyruvates. Additionally, we observed a high chemoselectivity for aromatic carbonyl systems. Comprehensive measurements were performed in this high-throughput experimental setup to gain important insights into the kinetics of hydrogenation reactions at the interface between heterogeneous and homogeneous catalysis.

Introduction

Although advanced strategies to optimize the activity of catalysts have been known for many decades, attention has shifted to control the selectivity for the desired product in catalysis research in recent years. This is related to an ecological focus, pollution control, and to develop green chemistry.[1,2] In this regard, the preparation of new catalysts, which combine homogeneous selectivity and heterogeneous recyclability, is of great interest in catalysis.[3,4] Furthermore, research aims towards new methods for the characterization of these catalysts to improve our understanding of catalysis in quasi-homogeneous systems.[5] The immobilization of catalysts in a two-phase system is one of the common technical solutions to achieve high chemoselectivity and to make the catalytic system recyclable.[1] With regard to industrial applications, metal nanoparticles offer many new opportunities because of their high surface area and, therefore, their high activity under mild reaction conditions. Based on the increased consumption of energy and decreasing fossil reserves, processes that involve the hydrogenation of CO and CO_2 receive much attention, for example, the optimization of Fischer–Tropsch synthesis to develop a selective processing of ordered hydrocarbons.[6] Established processes for gasoline synthesis mainly use Co and Fe catalysts. Ni and Ru catalysts are also known, especially for the production of high-molecular-weight hydrocarbons. Furthermore, Ru is the most active known Fischer–Tropsch catalyst, which is of considerable interest because of its efficiency at moderate temperatures of 150 °C.[7] Here we present highly active Ru nanoparticles for the selective hydrogenation of carbonyl groups. There have been various studies of the chemoselective hydrogenation of aromatic carbonyl systems.[8,9] Recently, Jiang and Zheng described the chemoselective hydrogenation reaction of aromatic aldehydes, ketones, and quinoline derivatives catalyzed by ionic-liquid-stabilized Ru nanoparticles.[8] In this study, we used our established strategy of on-column reaction gas chromatography (ocRGC) to investigate in detail the dependence of the catalyzed reaction on the temperature, the pressure of the reactive carrier gas (H_2), the catalyst loading, and the length of the active catalyst capillary. The utilization of the chromatographic technique described here allows us to perform high-throughput experiments and achieve the direct separation and quantification of the reaction mixture, which provides easy access to kinetic data and, therefore, improves our understanding of catalysis in quasi-homogeneous systems.[10–14] This experimental setup was already used by Trapp et al. for detailed studies of palladium.[15,16] There are various procedures to prepare, characterize, and apply Ru nanoparticles.[4] Somorjai et al. reported the synthesis of poly(vinylpyrrolidone)-stabilized Ru nanoparticles by the polyol reduction of $Ru(acac)_3$ (acac = acetylacetonate) and their use for CO oxidation.[17] Further suitable precursors are [Ru(cod)(cot)] (cod = 1,5-cyclooctadiene, cot = 1,3-cyclooctatetraene) or $RuCl_3$, which form small ligand- or polymer-stabilized Ru nanoparticles with a mean diameter of 1.5–6 nm. The protecting shell influences both the stability and the activity of the generated particles.[4,18] Several strategies have been applied for the stabiliza-

---

[a] *J. Gmeiner, Prof. Dr. O. Trapp*
Organisch-Chemisches-Institut
Ruprecht-Karls-Universität Heidelberg
Im Neuenheimer Feld 270, 69120 Heidelberg (Germany)
E-mail: trapp@oci.uni-heidelberg.de

[b] *Dr. S. Behrens*
Institut für Katalyseforschung und Technologie
Karlsruhe Institute of Technology
Herrmann-von-Helmholtz-Platz 1, 76344 Eggenstein-Leopoldshafen (Germany)

[c] *B. Spliethoff*
Max-Planck-Institut für Kohlenforschung
Kaiser-Wilhelm-Platz 1, 45470 Mülheim an der Ruhr (Germany)

Supporting information for this article is available on the WWW under http://dx.doi.org/10.1002/cctc.201501069.

tion of nanoparticles, which include the use of polymers, dendrimers, ligands, and ionic liquids.[19]

The concept presented here includes the in situ generation of highly active Ru nanoparticles stabilized by a polymer matrix for application in the selective hydrogenation reactions of carbonyl groups. [Ru(methylallyl)$_2$cod] was chosen as a suitable precursor for the preparation of the Ru nanoparticles. Recently, Prechtl et al. investigated this precursor in the hydrogenation of arenes under mild conditions (50–90 °C, 4 bar H_2). These Ru nanoparticles had a mean diameter of 2.1–3.5 nm and were stabilized using imidazolium ionic liquids.[20]

Results and Discussion

In this study, we prepared Ru nanoparticles by a method that has been established in our research group for the synthesis of Pd nanoparticles, in which a stabilizing polymeric matrix is obtained by using the copolymers methylvinyldimethylpolysiloxane (MVPS; 4.5 % $Si(O)(CH_3)(CH{=}CH_2)$ groups) and hydridomethyldimethylpolysiloxane (HMPS; 25.7 % $Si(O)(CH_3)H$ groups) that takes advantage of the metal as a hydrosilylation catalyst to promote the crosslinking of these copolymers.

The reduction of the Ru^{II} precursor [Ru(methylallyl)$_2$cod] is performed by the coordination of the Ru ions to the vinyl groups of MVPS (**1**) and the addition of HMPS (**2**). Consequently, the polymeric matrix is built up by the crosslinking Ru-catalyzed hydrosilylation reaction (Scheme 1).[15,16]

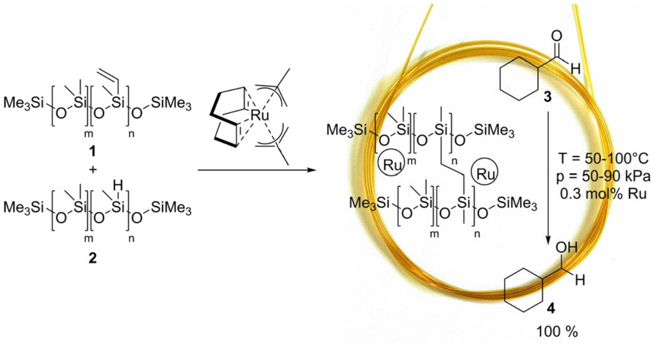

Scheme 1. Preparation of Ru nanoparticles embedded in a polymeric matrix for application in on-column reaction gas chromatography.[16] Full conversion was achieved for **3** by using a 50 cm long catalytic capillary (catalyst loading 0.3 mol % Ru).

The clear solution that contains the metal precursor and the mixture of the copolymers in anhydrous diethyl ether turns black within 2 h at room temperature, which corresponds to a fast reduction of the metal precursor. The Ru nanoparticles were characterized by high-resolution transmission electron microscopy (TEM). We observed spherical and crystalline particles with a narrow size distribution of (1.4 ± 0.2) nm. It can be seen from the TEM picture shown in Figure 1 that the particles are isolated separately in the polymeric matrix. As a result of the protecting polymer layer, no agglomeration was observed. The small size of the particles determined by TEM corresponds well with the high catalytic activity observed in the following hydrogenation experiments and will be discussed in detail (see Supporting Information).

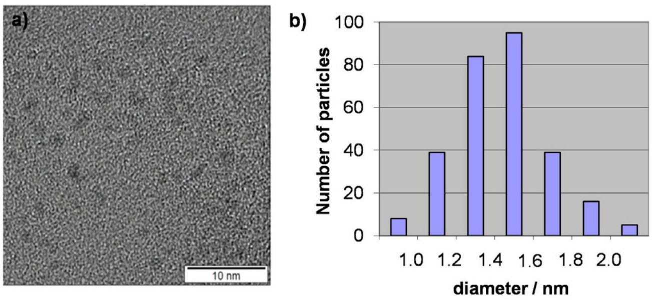

Figure 1. a) TEM image of the isolated Ru nanoparticles with a metal concentration of 1.0×10^{-7} mol mL^{-1}. Scale bar = 10 nm. b) Size distribution of the prepared Ru nanoparticles with a mean diameter of (1.4 ± 0.2) nm.

For the on-column GC measurements, a coating solution that contained 4 mg of the copolymers HMPS and MVPS and 33.4 µg of the Ru^{II} precursor in 1 mL diethyl ether was prepared to give a 250 nm film on the inner wall of the fused-silica capillary with an inner diameter of 250 µm (Scheme 1). The ratio of HMPS to MVPS was 3:1 to ensure an adequate concentration of HMPS for both the reduction of the metal ions and the formation of the stabilizing matrix as well as the immobilization to the capillary surface to achieve a stable film. Comprehensive studies of polymer-stabilized Pd nanoparticles for application in ocRGC prove that with this ratio no changes in the size and shape and no agglomeration of the particles were observed at elevated temperatures (200 °C) and after treatment with H_2. Therefore, we can conclude that the Ru catalyst embedded on the column shows similar characteristics as that in solution (Figure 1).[16]

The fused-silica capillaries were coated using the static method described by Grob[21] and then heated to 190 °C at a rate of 0.5 K min^{-1} under a slow stream of H_2 (10 kPa) to achieve the complete conversion of the reactants as well as a sufficient permanent bonding of the remaining Si–H groups to the capillary surface silanol groups. In previous studies of catalytically active capillaries coated with Pd nanoparticles, we added the slightly polar dimethyldiphenylpolysiloxane copolymer (GE-SE-52, 5 % phenyl groups) to improve the stability of the coating and the reproducibility of the on-column hydrogenation measurements.[16] Notably, we experienced a decrease in the catalytic activity of the Ru nanoparticles on the addition of GE-SE-52. The inhibiting effect in the on-column reaction chromatographic measurements can be explained by the stabilization of the nanoparticles and the shielding of the catalytically active sites.[22] The coated catalyst capillaries were installed between a preseparation column (GE-SE-30, 50 cm, i.d. 250 µm, 500 nm film thickness) and a separation column (GE-SE-52, 25 m, i.d. 250 µm, 250 nm film thickness) to integrate catalysis and analysis in a single experimental step (Figure 2).

The loading of Ru nanoparticles is calculated to be 2.1×10^{-13} mol cm$_{capillary}^{-1}$, which corresponds to a catalyst loading of 0.3 mol % using a 50 cm long catalytically active column. Hydrogen was used as the reactive carrier gas. A reactivation process was performed after each ocRGC experiment to sustain

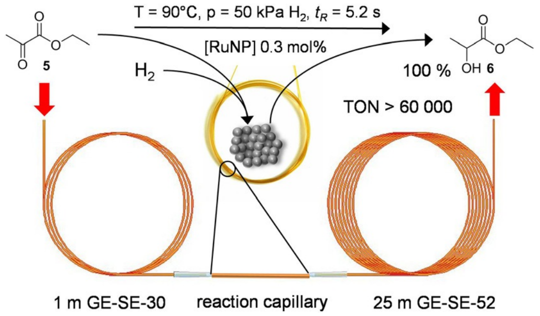

Figure 2. Experimental setup: The reaction capillary is coupled between a preseparation column (50 cm, GE-SE-30) and a separation column (25 m, GE-SE-52).

the reproducibility and activity of the catalyst column. Therefore, the capillary was heated to 160 °C at 40 kPa H_2 inlet pressure for 10 min. We observed the total conversion of cyclohexanecarboxaldehyde (**3**) in a broad temperature range (50–100 °C) at various inlet pressures (50–90 kPa) by using an only 50 cm long catalytically active column (Scheme 1). With regard to the extremely low reaction time of 5 s, which corresponds to the contact time of the substrate with the catalytically active column, we developed a nanoparticle-based catalyst system with a very high activity for the hydrogenation of carbonyl compounds.

Next we studied the hydrogenation reaction of ethylpyruvate (**5**) in detail (Figure 3). The dependence of the conversion on the length of the reactor capillary is shown in Figure 3 a. The conversion decreases with the length of the reactor capillary as expected because of the reduced contact time. The long-term stability of the catalytic capillaries was also examined. The microreactor can be reused over 200 times without a significant loss in conversion, which corresponds to a turnover number (TON) >60 000 (Figure 3 b). We monitored the dependence of the conversion on the temperature and the inlet hydrogen pressure to obtain a 3D dataset (Figure 3 c) that shows the expected trends, namely, high conversions at increased reaction temperatures and lower inlet pressures, which corresponds to increased reaction times. Here, conversions of up to 100 % were observed for reaction temperatures ≥80 °C. The effect of the decrease of the hydrogen pressure has only a minor influence on the conversion, which can be explained by a smaller impact on the contact time of the substrate with the catalytically active column. These observations confirm that the selectivity and activity of the Ru nanoparticles is mainly based on their nature, size, and stabilization in the polymeric matrix. This makes our high-throughput micro-flow-reactor system comparable with a classical batch reactor system and allows the fast reaction screening of various catalytic systems.[10–16]

We further investigated the activity of the Ru nanoparticle system in various hydrogenation reactions and studied their reaction kinetics. Based on the Langmuir–Hinshelwood mechanism, we calculated the activation parameters $\Delta G^{\neq}$, $\Delta H^{\neq}$, and $\Delta S^{\neq}$ as well as the reaction rate constants by using a first-order reaction rate law. The calculation was performed using temperature-dependent measurements. The activation enthalpy $\Delta H^{\neq}$ of the reaction was obtained from the slope, and the activation entropy $\Delta S^{\neq}$ was obtained from the intercept of the Eyring plot. Deviations were calculated by error-band analysis[16] of the linear regression.[23]

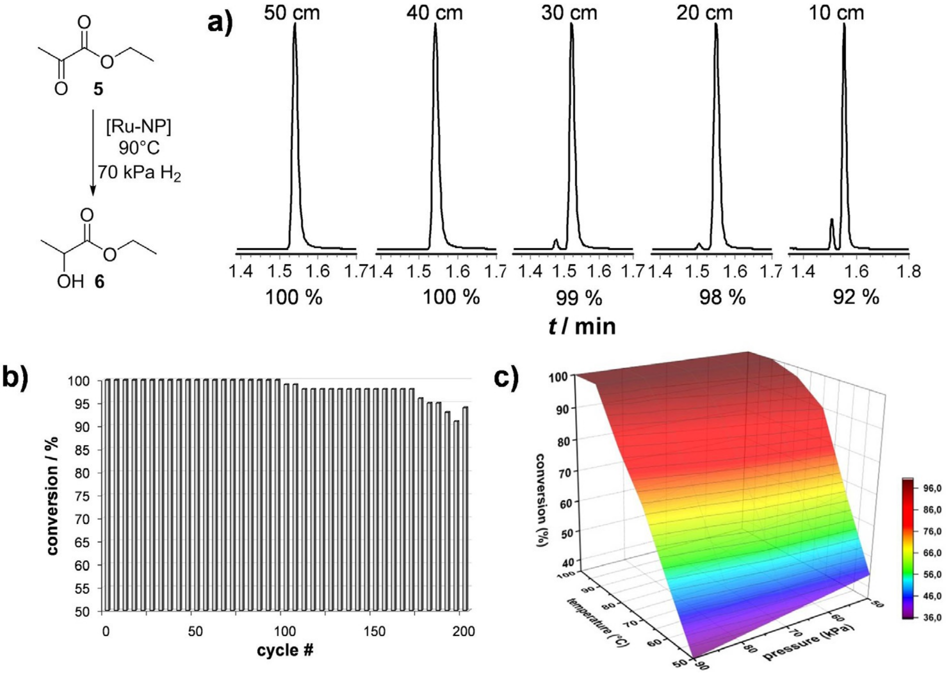

Figure 3. On-column hydrogenation reaction of **5**. a) Turnover dependent on the length of the catalyst capillary at 90 °C and 70 kPa H_2. b) Recyclability of Ru NPs for the hydrogenation of **5** at 90 °C and 70 kPa H_2 (catalyst loading 0.3 mol %). c) Three-dimensional dataset in the temperature range of 50–100 °C using inlet pressures of 50, 60, 70, 80, and 90 kPa H_2.

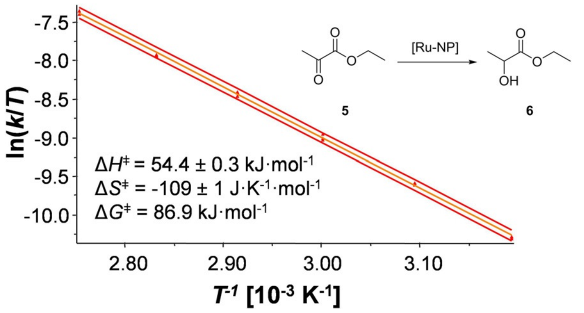

Figure 4. Eyring plot to determine the activation parameters of the hydrogenation reaction of **5** over Ru nanoparticles (catalyst loading 0.3 mol %).

The Eyring plot for the hydrogenation reaction of **5** obtained by temperature-dependent measurements is shown in Figure 4. The obtained low activation enthalpy $\Delta H^{\neq} = 54.4\,\mathrm{kJ\,mol^{-1}}$ and the highly negative entropy value $\Delta S^{\neq} = -109\,\mathrm{J\,mol^{-1}\,K^{-1}}$ corroborate the high catalytic activity and high temperature dependence of the hydrogenation reaction. In addition, the small error bands[16] demonstrate the high reproducibility and reliability of the hydrogenation measurements in the capillary-type microreactor employed here.

The systems studied in the hydrogenation reaction of carbonyl compounds are summarized in Table 1. We observed high conversions in a range of 90–100 % at moderate temperatures using a capillary catalyst loading of 0.3 mol %. A very low conversion of only 12 % for the aromatic ketone, acetophenone, was observed. It is well known that in this case a basic additive in the catalyst system is necessary for a chemoselective hydrogenation.[8,24] Recently, Jiang and Zheng described ionic-liquid-stabilized Ru nanoparticles and observed no catalytic activity without the addition of a base.[8] The Gibbs activation energy was in the range of 83.1 and 94.9 kJ mol^{-1}, which is in very good agreement with measurements of on-column hydrogenation reactions using metal nanoparticles performed previously.[16] The lowest activation energy of almost $\Delta G^{\neq} = 81\,\mathrm{kJ\,mol^{-1}}$ was determined for **3**, which explains the great activity for this system (Figure 1). For benzoylmethyl formate, a high $\Delta G^{\neq}$ value was determined as well, however, high conversions of up to 88 % were observed. These results can be explained by the very high retention of the substrate in the stationary phase of the catalytically active capillary, which is supported by the contact time of 30 s. In comparison, benzaldehyde has a reaction time of only 3 s.

Table 1. Results of the on-column hydrogenation measurements using Ru nanoparticles.

Substrate	C [%]	k[c] [10^{-1} s^{-1}]	$\Delta G^{\neq}$[d] [kJ mol^{-1}]	$\Delta H^{\neq}$ [kJ mol^{-1}]	$\Delta S^{\neq}$ [J mol^{-1} K^{-1}]
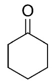	100[a]	3.5	83.1	39.5 ± 0.8	−146 ± 6
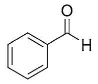	88[a]	3.5	83.3	39.6 ± 1.6	−147 ± 12
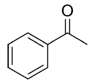	12[a]	0.05	94.9	55.2 ± 2.3	−132 ± 12
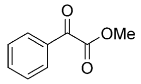	88[b]	0.9	93.0	52.6 ± 1.4	−135 ± 8
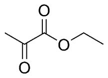	100[a]	–	86.9	54.4 ± 0.3	−109 ± 1
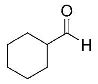	100[b]	–	81.7	34.1 ± 1.1	−135 ± 8

[a] Conversion C at 100 °C and 70 kPa using a catalyst loading of 0.3 mol %. [b] Conversion C at 90 °C and 70 kPa using a catalyst loading of 0.3 mol %. [c] Reaction rate constants reported at 90 °C and 70 kPa. [d] Gibbs activation energy at 25 °C.

Our results are in agreement with thermodynamic data for hydrogenation reactions of carbonyl compounds catalyzed homogenously published in the literature. For example, for the hydrogenation of cyclohexanone, we found an activation barrier of 83 kJ mol^{-1}, which is in very good agreement with the time-dependent measurements of the homogeneous hydrogenation reaction using the cationic complex $[\mathrm{RuH(CO)(NCMe)_2(PPh_3)_2}]^+$, in which a Gibbs activation energy of 85 kJ mol^{-1} was found.[25] This result demonstrates the suitability of ocRGC to study a catalytic system to determine activation parameters with high precision, and in this case, the quasi-homogeneous nature of the Ru nanoparticles.[26] At the interface of this homogeneous and heterogeneous system we are able to obtain the selectivity observed for homogeneous catalysis in the hydrogenation reaction of carbonyl compounds by the use of a heterogeneously immobilized catalyst.[1]

We further investigated the influence of *para* substituents in the chemoselective hydrogenation of benzaldehyde (Figure 5). Although Jiang et al. observed a strong solvent dependence in their studies of ionic-liquid-stabilized Ru nanoparticles,[8] we observed a 100 % chemoselective conversion with a catalyst loading of 0.3 mol %. Moreover, we noticed a small influence of the substituent.[27] As expected, an electron-withdrawing group has a positive impact on the reaction, whereas electron-donating groups lead to a decreased conversion. This effect was also seen by substitution in the α-positions. We already mentioned that a basic additive is required for the hydrogenation of acetophenone, however, the conversion for trifluoroacetophenone increases significantly, which can be attributed to the electron-withdrawing substitution. As a result of the electron-donating influence in phenyl formate, we observe again a decreased conversion compared with the unsubstituted benzaldehyde.

An increase of the catalyst loading to 0.6 mol % led to an increased activity and an almost 100 % chemoselective conversion for all substrates studied (Figure 6 b). The obtained TEM picture of a Ru loading of

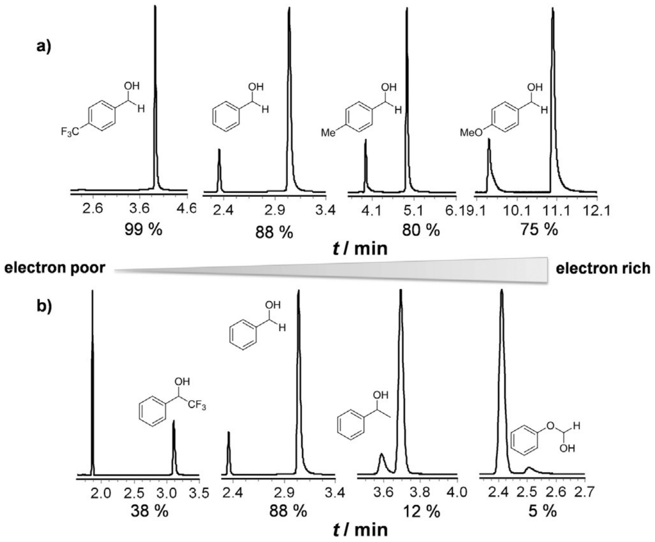

Figure 5. a) Influence of *para* substitution on the chemoselective hydrogenation reaction of benzaldehyde. b) Influence of substitution in the α-position.

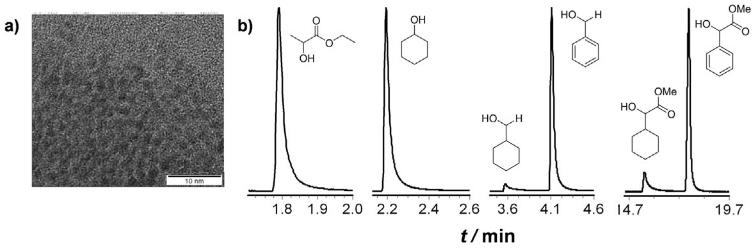

Figure 6. Doubled catalyst loading of 2.1×10^{-7} mol mL^{-1}. a) TEM image of the Ru nanoparticles. Scale bar = 10 nm. b) Elution profiles of the studied substrates with the use of a 50 cm catalytically active column (catalyst loading 0.6 mol% Ru) at 90 °C and 70 kPa H_2.

2.1×10^{-7} mol mL^{-1} shows a higher concentration of particles with a comparable mean diameter of (1.4 ± 0.2) nm (Supporting Information). The increased number of particles were no longer embedded separately in the polymer matrix, but no aggregation was observed (Figure 6a). The prepared catalyst column shows a high activity in the selective carbonyl hydrogenation, whereas the aromatic system is hydrogenated to a lower extent. These results confirm that the particles maintain the expected quasi-homogeneous behavior and the desired chemoselectivity in the studied reaction if the number of available catalytically active Ru sites is increased.[28]

Conclusions

In this study we presented the preparation of Ru nanoparticles for chemoselective hydrogenation reactions under mild reaction conditions. By the use of the well-established technique of on-column reaction chromatography we were able to study these reactions in a high-throughput experimental setup in detail. The obtained insights into quasi-homogeneous carbonyl compound hydrogenation, which combined the reusability of the heterogeneously coated catalyst and the selectivity of homogeneous systems in a capillary microreactor, offer great potential for the examination of various industrially relevant processes.

Experimental Section

Coating of fused-silica columns

[Ru(methylallyl)$_2$cod] (0.1 mg), HMPS (9 mg), and MVPS (3 mg) were dissolved in anhydrous diethyl ether (3.00 mL). The fused-silica capillary (i.d. 250 μm) was coated by the static method described by Grob[21] using this solution to give a 250 nm film on the inner wall of the capillary. Immobilization was achieved under a stream of H_2 (10 kPa) using a temperature program starting at 40 °C for 10 min then heating to 190 °C for 10 h at a rate of 0.5 K min^{-1}.

On-column reaction gas chromatographic hydrogenation measurements

The hydrogenation measurements were performed by on-column reaction gas chromatography. The catalyst capillary (10–50 cm) was coupled between a preseparation column, coated with GE-SE-30 (50 cm, i.d. 250 μm, 500 nm film thickness), and a separation column, coated with GE-SE-52 (25 m, i.d. 250 μm, 250 nm film thickness). H_2 was used as the reactive carrier gas. All measurements were repeated three times at each temperature and pressure. After each measurement the column was reactivated at 160 °C and 40 kPa H_2 for 10 min.

Acknowledgements

This work was supported by the European Research Council under Grant Agreements No. StG 258740 (AMPCAT).

Keywords: heterogeneous catalysis · high-throughput screening · homogeneous catalysis · hydrogenation · nanoparticles

[1] D. Astruc, F. Lu, J. R. Aranzaes, *Angew. Chem. Int. Ed.* **2005**, *44*, 7852–7872; *Angew. Chem.* **2005**, *117*, 8062–8083.
[2] J. Grunes, J. Zhu, G. A. Somorjai, *Chem. Commun.* **2003**, 2257.
[3] J. A. Gladysz, *Chem. Rev.* **2002**, *102*, 3215–3216.
[4] P. Lara, K. Philippot, B. Chaudret, *ChemCatChem* **2013**, *5*, 28–45.
[5] G. A. Somorjai, K. McCrea, *Appl. Catal. A* **2001**, *222*, 3–18.
[6] H. Schulz, *Appl. Catal. A* **1999**, *186*, 3–12.
[7] a) M. Vannice, *J. Catal.* **1975**, *37*, 462–473; b) H. Pichler, H. Buffleb, *Brennst.-Chem.* **1940**, *21*, 273–280.
[8] H.-y. Jiang, X.-x. Zheng, *Catal. Sci. Technol.* **2015**, *5*, 3728–3734.
[9] a) F. Jutz, J.-M. Andanson, A. Baiker, *J. Catal.* **2009**, *268*, 356–366; b) D. Gonzalez-Galvez, P. Lara, O. Rivada-Wheelaghan, S. Conejero, B. Chaudret, K. Philippot, P. W. N. M. van Leeuwen, *Catal. Sci. Technol.* **2013**, *3*, 99.
[10] S. Stockinger, O. Trapp, *Beilstein J. Org. Chem.* **2013**, *9*, 1837–1842.
[11] H. Cousin, O. Trapp, V. Peulon-Agasse, X. Pannecoucke, L. Banspach, G. Trapp, Z. Jiang, J. C. Combret, V. Schurig, *Eur. J. Org. Chem.* **2003**, 3273–3287.
[12] J. Gmeiner, M. Seibicke, C. Lang, U. Gärtner, O. Trapp, *Adv. Synth. Catal.* **2014**, *356*, 2081–2087.
[13] S. Stockinger, J. Gmeiner, K. Zawatzky, J. Troendlin, O. Trapp, *Chem. Commun.* **2014**, *50*, 14301–14309.

[14] J. Troendlin, J. Rehbein, M. Hiersemann, O. Trapp, *J. Am. Chem. Soc.* **2011**, *133*, 16444 – 16450.

[15] O. Trapp, S. K. Weber, S. Bauch, W. Hofstadt, *Angew. Chem. Int. Ed.* **2007**, *46*, 7307 – 7310; *Angew. Chem.* **2007**, *119*, 7447 – 7451.

[16] O. Trapp, S. K. Weber, S. Bauch, T. Bäcker, W. Hofstadt, B. Spliethoff, *Chem. Eur. J.* **2008**, *14*, 4657 – 4666.

[17] S. H. Joo, J. Y. Park, J. R. Renzas, D. R. Butcher, W. Huang, G. A. Somorjai, *Nano Lett.* **2010**, *10*, 2709 – 2713.

[18] a) C. Pan, K. Pelzer, K. Philippot, B. Chaudret, F. Dassenoy, P. Lecante, M.-J. Casanove, *J. Am. Chem. Soc.* **2001**, *123*, 7584 – 7593; b) D. González-Gálvez, P. Nolis, K. Philippot, B. Chaudret, P. W. N. M. van Leeuwen, *ACS Catal.* **2012**, *2*, 317 – 321.

[19] a) C.-J. Jia, F. Schüth, *Phys. Chem. Chem. Phys.* **2011**, *13*, 2457 – 2487; b) Q. M. Kainz, O. Reiser, *Acc. Chem. Res.* **2014**, *47*, 667 – 677; c) S. Noël, B. Léger, A. Ponchel, K. Philippot, A. Denicourt-Nowicki, A. Roucoux, E. Monflier, *Catal. Today* **2014**, *235*, 20 – 32; d) L. M. Martinez-Prieto, C. Urbaneja, P. Palma, J. Campora, K. Philippot, B. Chaudret, *Chem. Commun.* **2015**, *51*, 4647 – 4650.

[20] a) M. H. G. Prechtl, P. S. Campbell, J. D. Scholten, G. B. Fraser, G. Machado, C. C. Santini, J. Dupont, Y. Chauvin, *Nanoscale* **2010**, *2*, 2601; b) M. H. G. Prechtl, M. Scariot, J. D. Scholten, G. Machado, S. R. Teixeira, J. Dupont, *Inorg. Chem.* **2008**, *47*, 8995 – 9001.

[21] K. Grob, *Making and manipulating capillary columns for gas chromatography*, Hüthig, Heidelberg, **1986**.

[22] J. Kobayashi, Y. Mori, K. Okamoto, R. Akiyama, M. Ueno, T. Kitamori, S. Kobayashi, *Science* **2004**, *304*, 1305 – 1308.

[23] O. Trapp, *Anal. Chem.* **2006**, *78*, 189 – 198.

[24] T. Ohkuma, H. Ooka, S. Hashiguchi, T. Ikariya, R. Noyori, *J. Am. Chem. Soc.* **1995**, *117*, 2675 – 2676.

[25] M. Rosales, Á. González, M. Mora, N. Nader, J. Navarro, L. Sánchez, H. Soscún, *Trans. Met. Chem.* **2004**, *29*, 205 – 211.

[26] S. Vukojević, O. Trapp, J.-D. Grunwaldt, C. Kiener, F. Schüth, *Angew. Chem. Int. Ed.* **2005**, *44*, 7978 – 7981; *Angew. Chem.* **2005**, *117*, 8192 – 8195.

[27] L. Song, X. Li, H. Wang, H. Wu, P. Wu, *Catal. Lett.* **2009**, *133*, 63 – 69.

[28] J. Julis, M. Hölscher, W. Leitner, *Green Chem.* **2010**, *12*, 1634.

Received: September 30, 2015